Summary

In this chapter, nanostructured phosphomolybdate solid templated by a cationic surfactant, cetyltrimethylammonium bromide (CTAB) was synthesized and characterized by PXRD, FTIR, FESEM and EDAX analysis. The thermal stability of the solid was established using TGA. Further, the potential of the synthesized solid in removing cationic and anionic dyes form aqueous solution was investigated and it was found that the solid had high adsorption capacity for removing cationic dyes. Langmuir and Freundlich isotherm models were applied to the experimental data to find the suitable model for describing the adsorption equilibrium. The adsorption kinetics were also evaluated using pseudo-first order, pseudo-second order and intra-particle diffusion models.

V.1 Introduction

Pollution is one of the major global concerns and has serious consequences on the environment, human health, and the planet as a whole. In particular, pollution due to dyes is a significant environmental issue that affects the air, water, and soil in several parts of the world [1]. Dyes are used in a variety of industries, including textiles, leather, printing and cosmetics, to produce bright and vibrant colors. However, the release of dye effluent from factories is often discharged directly into rivers and lakes, contaminating these water bodies and making them toxic to aquatic life. In addition, dyes can bind to organic matter and sediments, causing them to sink to the bottom of water bodies and suffocating plant and animal life. This not only affects the immediate area, but also has wider implications for the entire ecosystem, as the food chain is disrupted and toxic substances are spread through the water [2,3]. Therefore, it is important to prevent or minimize the release of harmful dyes to protect the balance and tranquilly of the environment, particularly of aquatic ecosystems.

Researchers from all over the world have made significant attempts to regulate water pollution, and a number of approaches have been suggested in literature. Some of these include coagulation, ion-exchange, photocatalysis, solvent extraction, chemical oxidation, adsorption, electrolysis, etc. [4-8]. Because of its convenience, ease of use, and simplicity of design, the adsorption process is preferred above other techniques currently available for controlling water pollution [9]. Adsorbents that are commonly used to treat dye contaminated water include zeolites [10], activated carbon [11], agro waste [12], clay [13], etc. However, these materials have poor selectivity and limited adsorption capacity. Hence, developing more suitable and efficient materials for removing dyes is vital. In this regard, surfactant templated polyoxometalate (POM) hybrid solids have been explored as novel adsorbents for removal of dye by a few researchers. For instance, Yao *et.al.* has

reported a Keggin type POM *viz.* decamolybdodivanadophosphate ($H_5[PV_2Mo_{10}O_{40}]$) encapsulated by a cationic surfactant dimethyldioctadecylammonium bromide as an efficient adsorbent for removal of Reactive black 5 dye [14].

Therefore, in this chapter, an attempt was made to synthesize phosphomolybdate (a POM) solid templated by a cationic surfactant *viz.* cetyltrimethylammonium bromide (CTAB) and investigate its potential as an adsorbent for removing cationic and anionic dyes from aqueous solution. The effect of adsorbent dosage, contact time and initial dye concentration on the removal efficiency was studied. In addition, various isotherm and kinetic models were also investigated in order to better understand the adsorption behavior. The results are significant as most of the works on surfactant-POM hybrids is limited to structural studies and only a few examples of their potential use as catalytic materials, pH probes and electro/photochromic properties have been reported [15-17]. These materials also offer a way to investigate the self-assembly behaviour of phosphomolybdate (PMO) hybrid solids [18-22]. Surfactants can act as an ideal structure-directing agent for forming lamellar type PMOs via self-assembly approach [23,24]. In addition, the morphology and properties of surfactant-PMO solids can be tuned by varying the chain length, size and shape of the surfactant molecules resulting in amorphous or crystalline solids ranging from nano to micro dimensions [25-27].

V.2 Experimental

V.2.1 Synthesis of CTAB templated phosphomolybdates

The synthesis was carried out similar to the procedure reported by Thomas.*et.al.*[22]. Initially two different solutions were prepared. Solution A was prepared by dissolving $Na_2MoO_4{\cdot}2H_2O$ (0.30 g, 1.25 mmol) in 20 mL of water. Solution B was prepared by dissolving CTAB (0.08 g, 0.31 mmol) in 10 mL of water. Subsequently, solution A was added slowly to solution B with vigorous stirring, followed by adding 1M H_3PO_4

dropwise till the pH of the solution was ~1. Immediately, white precipitate was formed which gradually turned to yellow after stirring for 24 hours. Thereafter, it was left undisturbed for two days. Finally, a yellow-colored precipitate was obtained. It was washed with water and ethanol and dried in air. Scheme V.1 shows the experimental procedure for synthesis.

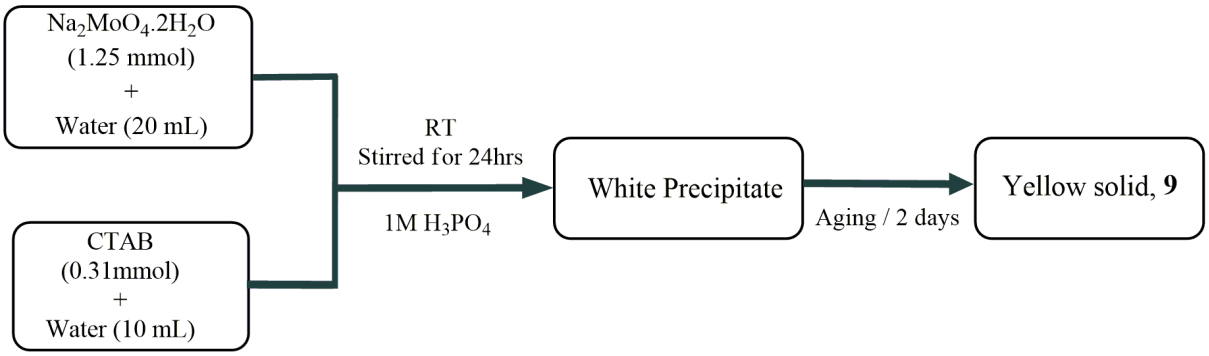

Scheme V.1 Synthetic procedure for preparing CTAB templated phosphomolybdates.

V.2.2 Preparation of dye stock solutions

A stock solution (50 ppm) of methylene blue (MB), malachite green (MG), methyl orange (MO) and eosin Y (EY) was prepared by dissolving 50mg of it in 1L of distilled water. The stock solution was diluted for further studies.

V.2.3 Dye removal studies

A series of batch adsorption experiments were conducted to determine the adsorption of dyes on the PMO solid, **9**. All the batch adsorption experiments were performed on a magnetic stirrer using 100 mL beaker containing 25mL each of dye solutions of pH 7.0±0.1. Experiments were performed at 27°C (300 K). All solution samples post adsorption were filtered through Whatman No:1 filter paper. The concentrations of dye in

treated samples were determined by measuring the absorbance using UV-visible spectrophotometer (Shimadzu UV-1800).

The amount of dye adsorbed per unit mass of the adsorbent was evaluated by using the following equation,

$$Qt = \frac{C_0 - C_t}{M} \times V$$

where,

C_0 = Initial concentration of dye (mg/L)

C_t = Liquid phase concentration of dye at any time (mg/L)

V = Volume of dye took for adsorption, in ml

M = Weight of adsorbent dose, in g.

The percentage of dye removed was calculated by the following equation,

$$\% \text{ Removal} = \frac{(C_o - C_t)}{C_o} \times 100$$

V.2.4 Modeling of adsorption isotherms and its studies

In order to optimize the design of a sorption system to remove dyes from aqueous solutions, it is important to establish the most appropriate correlations for the equilibrium curves. The Langmuir and Freundlich isotherms are widely applied to adsorption processes.

(a) Langmuir isotherm

The most widely used isotherm equation for modeling of the adsorption data is the Langmuir equation, which is valid for monolayer sorption onto a surface with a finite number of identical sites and is given by following equation,

$$q_e = \frac{Q_{max}\ b_L\ Ce}{1 + b_L\ Ce}$$

For solid - liquid systems, the Langmuir isotherm is expressed in the linear form as [28]:

$$\frac{Ce}{qe} = \frac{1}{Q_{max}\ bL} + \frac{Ce}{Q_{max}}$$

where,

q_e = The amount of dye adsorbed per gram of the adsorbent at equilibrium

Q_{max} = monolayer adsorption capacity, (mg/g), signifies the solid phase concentration, corresponding to the complete coverage of available sorption site, can be evaluated from the slope of Langmuir isotherm plot (Ce/qe against Ce)

C_e = The equilibrium concentration of adsorbate (mg/L)

b_L = Langmuir Isotherm constant (L/g). This value corresponds to energy of sorption, calculated from the intercept of the linear plot of Langmuir isotherm.

The best-fit equilibrium model was determined based on the linear squared regression correlation coefficient R^2. The dimensionless separation factor R_L describes the type of isotherms and is defined by,

$$R_L = \frac{1}{1 + bCo}$$

where,

b is Langmuir constant

C_o is the adsorbate initial concentration.

The parameters indicate the shape of the isotherm accordingly, if, R_L value lies in between 1 to 0, then favorable adsorption indicated. If, R_L value greater than 1, unfavorable adsorption, while a value of 1 represents linear & unfavorable and 0 represents irreversible.

(b) Freundlich isotherm

The Freundlich isotherm model is derived by assuming a heterogeneous surface with a non-uniform distribution of heat of adsorption over the surface, the Freundlich model in non-linear & linear form can be expressed as [29],

$$q_e = = K_F (Ce)^{1/n}$$

$$\log q_e = \log K_F + \frac{1}{n} \log Ce$$

where,

K_F is the Freundlich characteristics constant and 1/n the heterogeneity factor of adsorption, obtained from intercept and slope of $\ln(q_e)$ vs $\ln(C_e)$ linear plot respectively.

K_F and n are the physical constants of Freundlich adsorption isotherm which indicate the adsorption capacity and adsorption intensity, respectively.

If n =1, then the partition between the two phases is independent of the concentration. 1/n <1 indicate normal adsorption, 1/n >1 indicate cooperative adsorption and 1/n =1 is the linear adsorption isotherm.

V.2.5 Adsorption Dynamics

Kinetics is of great significance to evaluate the performance of a given adsorbent and gain insight into the underlying mechanisms. Solute uptake rate determines the residence time required for completing the adsorption reaction and can be enumerated from kinetic analysis. The kinetics of sorption that defines the efficiency of sorption of Methylene Blue dye was checked by the pseudo-first order, pseudo-second order and intra-particle diffusion models.

(a) Pseudo-First Order Model

The pseudo-first order rate expression of Lagergren model is generally expressed as follows [30]:

$$\frac{dq}{dt} = k_1 (q_e - q)$$

where,

q_e and q are the amounts of adsorbed dye (mg/g) onto the adsorbent at equilibrium and at time t (min), respectively

k_1 is the rate constant of first-order adsorption.

The linear form of the above equation can be obtained as:

$$\log (q_e\text{-}q) = \log q_e - k_1 \left(\frac{t}{2.303} \right)$$

The plot of $\log(q_e\text{-}q)$ against t for the pseudo-first order equation gives a linear relationship and k_1 and q_e values can be determined from the slope and intercept of this equation, respectively.

(b) Pseudo-Second Order Model

The differential form of the pseudo-second order equation can be represented as [31]:

$$\frac{dqt}{dt} = K_2 (q_e - q_t)^2$$

where,

K_2 is the pseudo-second order rate constant (g/mg/min).

The linear form of the above equation can be obtained by integration of the equation for the boundary conditions $q_t = 0$ at t=0 and $q_t = q_t$ at t=t,

$$\frac{t}{q_t} = \frac{1}{K_2 qe^2} + \frac{t}{q_e}$$

A plot of $t/q_{t\ versus}$ t gives a straight line with slope $1/q_e$ and intercepts $1/k_2q_e$.

The initial Sorption rate, h (mg/g.min), at t ⟶0 is defined as:

$h = K_2 q_e^2$

(c) Intra-particle Diffusion Model

The intra-particle diffusion model was proposed by Weber and Morris to identify the diffusion mechanism of the adsorption process [32]. Intra-particle diffusion is a transport process involving movement of species from the bulk of the solution to the solid phase. A plot of the amount of sorbate adsorbed, q_t (mg/g) and the square root of the time, gives the rate constant (slope of the plot). It is calculated by using the intra-particle diffusion model [32] given as,

$$q_t = K_{diff}\, t^{1/2} + C$$

where,

q_t is the amount of dye adsorbed (mg/g) at time t.

C is the boundary layer thickness

K_{diff} is the intra-particle diffusion rate constant (mg/g/min)

The plot of the amount dye adsorbed, q_t versus $t^{1/2}$ will give a straight line with a slope of K_{diff} and an intercept of C.

V.3 Characterization

The synthesized CTAB templated PMO nanoparticles, **9** were characterized by techniques namely PXRD, FTIR and TGA as discussed under Section II.2.3 in chapter II. Field emission scanning electron microscopy studies (FESEM) and Energy dispersive X-ray analysis (EDAX) were carried out using Gemini SEM 300 (Carl Zeiss).

V.4 Results and Discussion

V.4.1 Characterization of CTAB templated PMO nanoparticles, 9

The PXRD pattern of **9** (Figure V.1a) showed broad *00l* reflections which indicated lamellar characteristics, with a d-spacing ~ 3.5 nm. FTIR of the synthesized PMO solid showed the presence of strong bands around 1068 cm^{-1} due to PO_4 groups, peaks around 881 and 613 cm^{-1} were attributed to Mo=O and Mo-O vibrations. Two absorption peaks at 2926 and 2850 cm^{-1} corresponded to the C-H stretching vibrations of methyl and methylene groups of CTAB. Peak at 1473 cm^{-1} were attributed to C-H bending vibrations of CTAB moiety as shown in Figure V.1b. The morphology and composition of the synthesized PMO solid was analyzed using FESEM and EDAX analysis. FESEM images indicated a spherical morphology with particle size varying from 78 to 167 nm (Figure V.2a). EDAX spectrum showed the peaks corresponding to carbon, nitrogen, phosphorus, molybdenum and oxygen (Figure V.2b). TGA showed weight loss in the temperature region 290-400°C due to the decomposition of CTAB moieties incorporated in the Mo-O-P framework. The amount of CTAB present in the sample was estimated to be ~ 30%. The second weight loss occurred after 400°C due to the decomposition of the phosphomolybdate anion and a residual mass of 55% was obtained at 800°C. On the basis of TGA and EDAX, the composition was found to be $(CTAB)PMoO_6$.

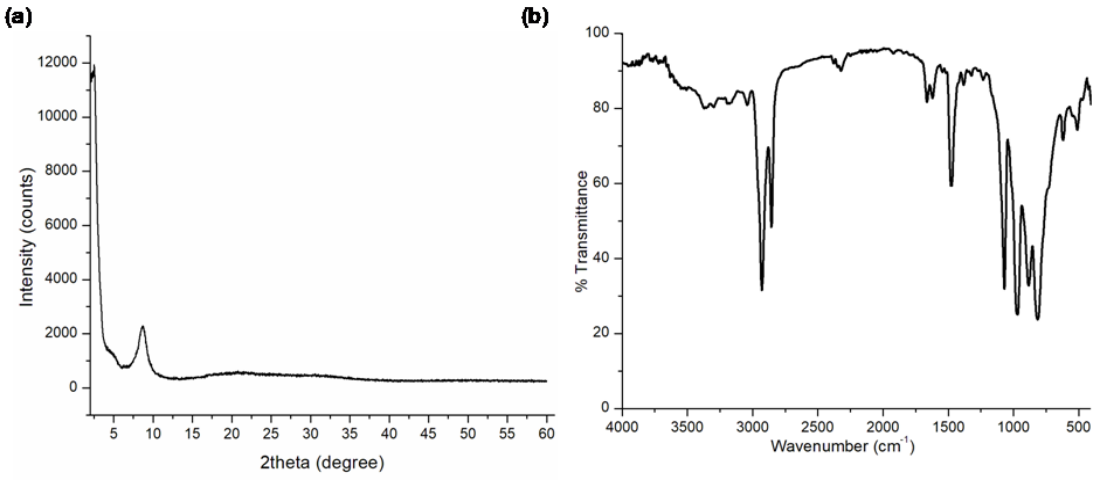

Figure V.1 (a) PXRD and (b) FTIR of solid **9**.

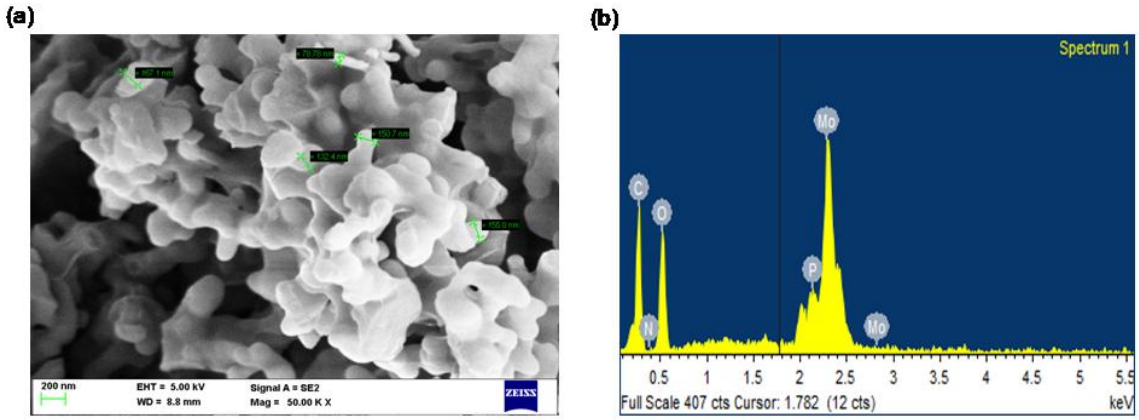

Figure V.2 (a) FESEM and (b) EDAX spectrum of solid **9**.

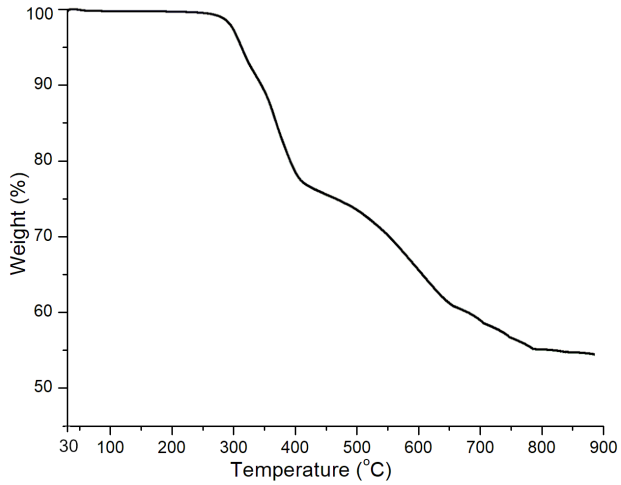

Figure V.3 TGA plot of solid **9**.

V.4.2 Dye removal studies

The dye adsorption behavior of **9** was investigated by using methylene blue (MB) as the model dye. It was observed that **9** could effectively remove MB from the aqueous solution as shown in Figure V.4. The effect of various parameters such as adsorbent dosage, contact time, initial dye concentration and reusability of **9** for the removal of MB was further investigated. The nature of dye was also examined by using other dyes.

V.4.2.1 Effect of adsorbent dosage

The effect of adsorbent dosage was studied by varying the amount of **9** from 0.02 to 0.1g for the removal of MB dye. 25 mL of 5 ppm MB solutions containing varying amounts of adsorbents were stirred for 20 minutes. From Figure V.5, it can be inferred that an increase in the amount of solid **9**, more dye moieties could be removed from dye contaminated water. The maximum removal efficiency was observed with a dosage of 0.1g of **9**. A further increase in the amount of **9** showed no significant increase in the dye removal.

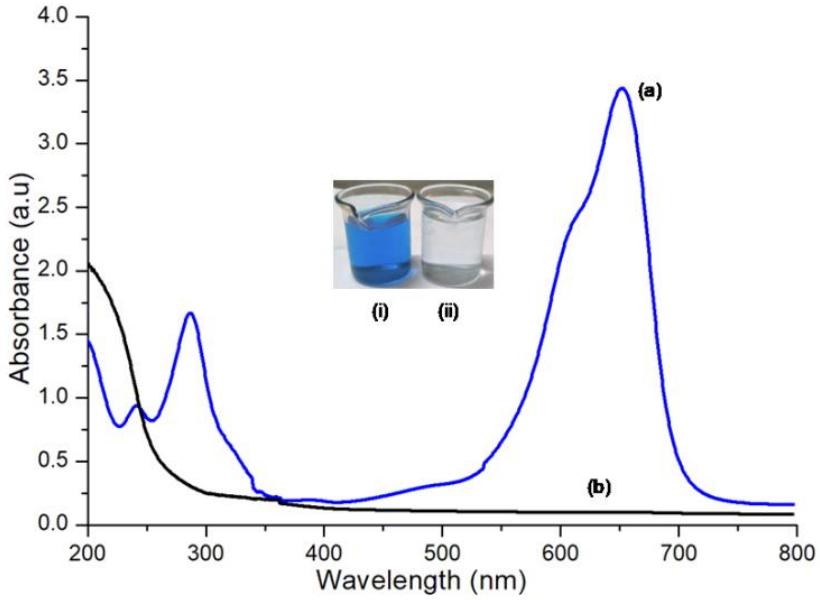

Figure V.4 UV-Visible spectra of (a) solution of 5ppm MB and (b) MB solution obtained after treatment with **9** for 1 hour. Figures in the inset represent (i) the original solution of MB and (ii) MB solution obtained after treatment with **9** for 1 hour.

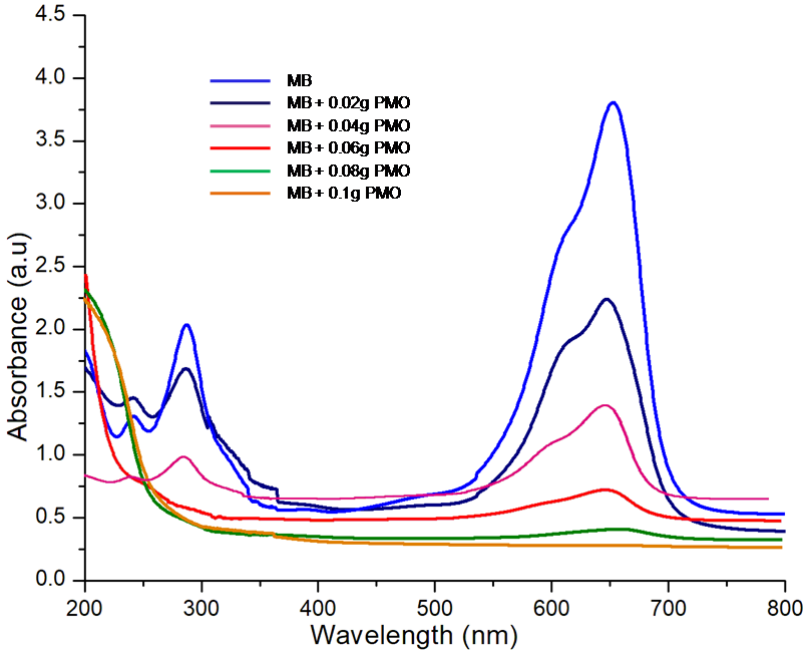

Figure V.5 UV-visible absorption spectra of MB (5 ppm, 25 mL) solution showing the effect of dose on dye removal upon stirring for 20 minutes.

V.4.2.2 Effect of contact time

The effect of contact time on the dye removal efficiency was also investigated using 25 mL of 5 ppm MB solution containing 0.1g of **9**. The solution was stirred and absorbance was measured at regular time intervals (10, 20, 30, 40, 50 and 60 minutes). Figure V.6 shows the effect of contact time with respect to MB removal efficiency. From the figure it can be observed that MB removal increased with increase in time and a maximum removal was achieved at 40 minutes of stirring. After 40 minutes, the efficiency of adsorption process did not change significantly, which could indicate the equilibrium adsorption of the MB dye. Therefore, the equilibrium time for the MB dye adsorption process was found to be 40 minutes.

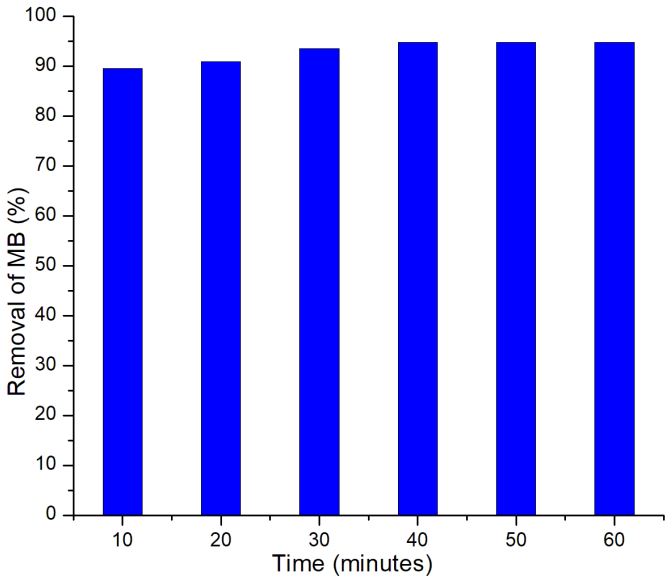

Figure V.6 Effect of contact time on MB dye removal by **9**.

V.4.2.2 Effect of initial dye concentration

The initial concentration of dye has a significant impact on the adsorption process since it provides the necessary driving force for mass transfer between the aqueous phase (aqueous solution containing dye) and the solid phase (adsorbent). Hence, the effect of initial concentration of MB on the adsorption process was studied by varying the

concentration of MB. Figure V.7 shows the effect of the initial concentration of MB dye in the range of 3–8 ppm on the efficiency of dye removal at a PMO dosage of 0.1g and contact time of 40 minutes. It was observed that the percentage removal of dye sharply increased from 77% to 95% on increasing the initial dye concentration from 3ppm to 5 ppm. Further increase in the MB dye concentration caused a decrease in the adsorption efficiency as seen in Figure V.7. An increase in the removal efficiency at low concentrations of dye solution could be due to the greater interaction of dye molecules with the surface and active sites in the solid, **9**. However, a decrease in the dye removal efficiency at high dye concentrations could be attributed to the saturation of active sites in the solid, **9** at high concentrations of MB solution.

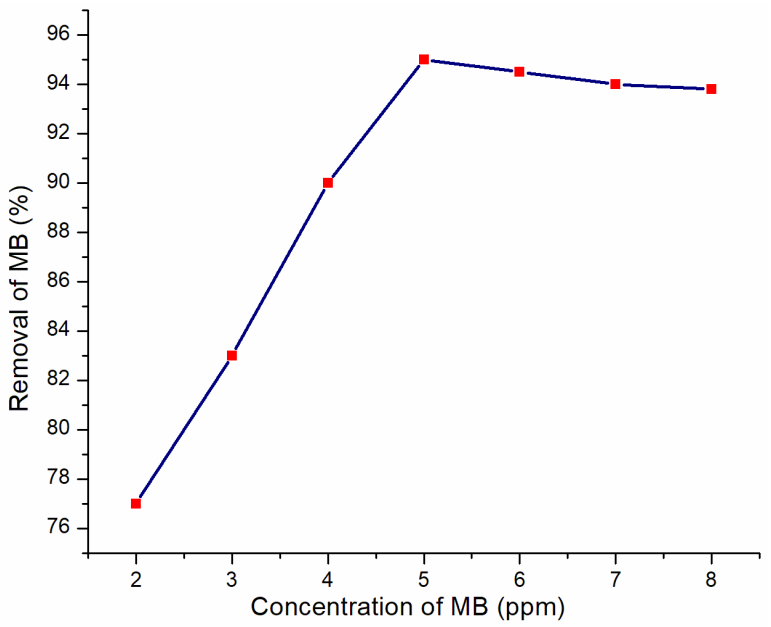

Figure V.7 Effect of initial concentration of MB on the adsorption process.

V.4.2.3 Effect of the nature of dye

Apart from MB dye, the effectiveness of **9** in removing other dyes viz; malachite green (MB), methyl orange (MO) and eosin Y (EY) was also examined for a clear insight of the adsorption mechanism. 0.1g of adsorbent was added to each of the dye solutions (25 mL, 5 ppm) and stirred for 40 minutes. The initial and final absorbance was measured using UV-visible spectrophotometer. Figure V.8 shows the absorption spectra of dyes before and after treating with **9**. It was observed that **9** could effectively remove malachite green (MG) similar to that of MB. On the other hand, the absorption spectra of anionic dyes viz; MO and EY after treating with **9** did not show any significant decrease in its intensity as observed in Figure V.8. Hence, it can be inferred that the synthesized solid, **9** was more effective in removing only the cationic dyes.

V.4.2.3 Reusability of CTAB-PMO solid

One of the crucial factors in the wastewater treatment process is the adsorbent's capacity to be reused and recovered. Solid **9** after treatment with the MB dye solution was filtered, washed with water and air dried. It was then retested for its adsorption efficiency in removing MB dye solution upto 10 cycles. Figure V.9 shows that there is no decrease in the percentage of removal of MB upto 6 consecutive cycles. However, a decrease in the percentage of removal of dye was observed in later cycles.

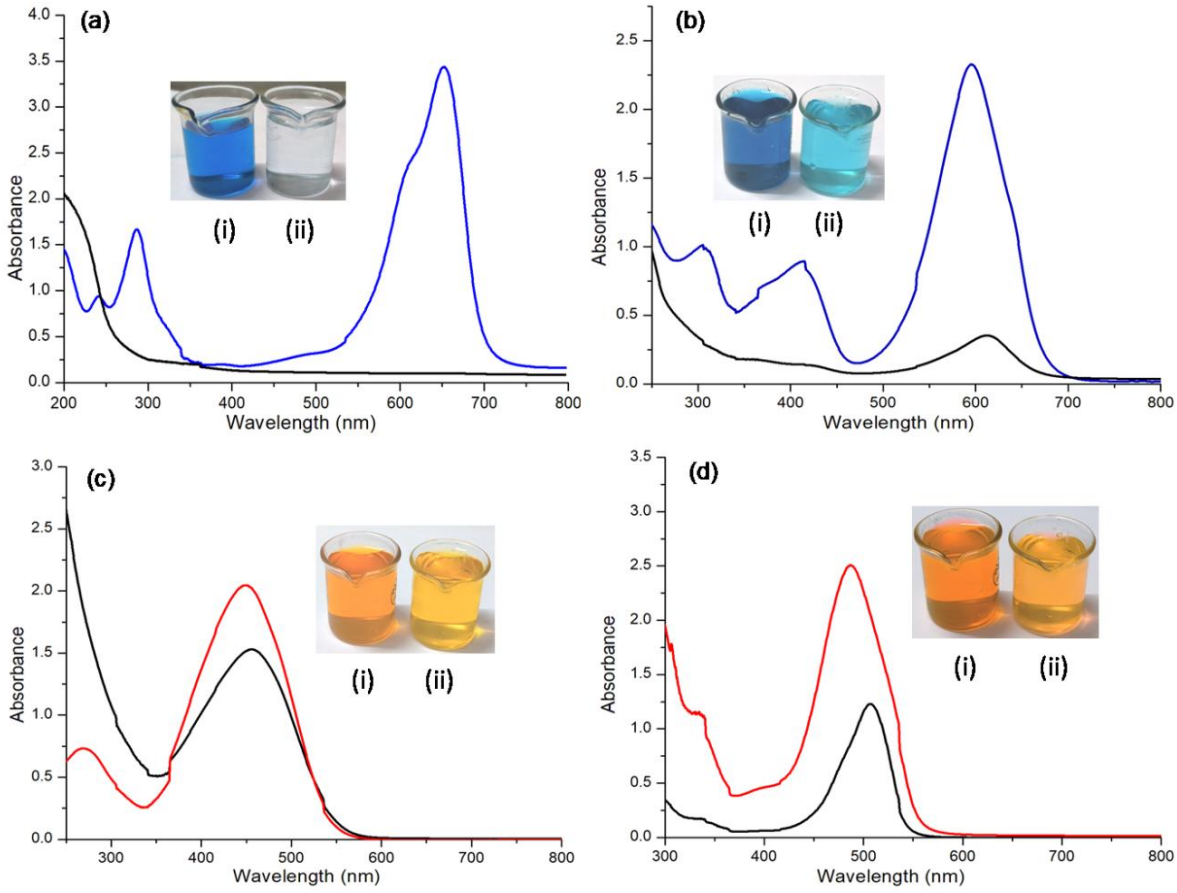

Figure V.8 UV-Visible spectra of 5ppm dye solutions (a) MB, (b) MG, (c) MO and (d) EY before (colored curve) and after (black curve) treating with 0.1g of **9**. Image in the inset represents (i) the original dye solution and (ii) dye solution obtained after treatment with **9** for 40 minutes.

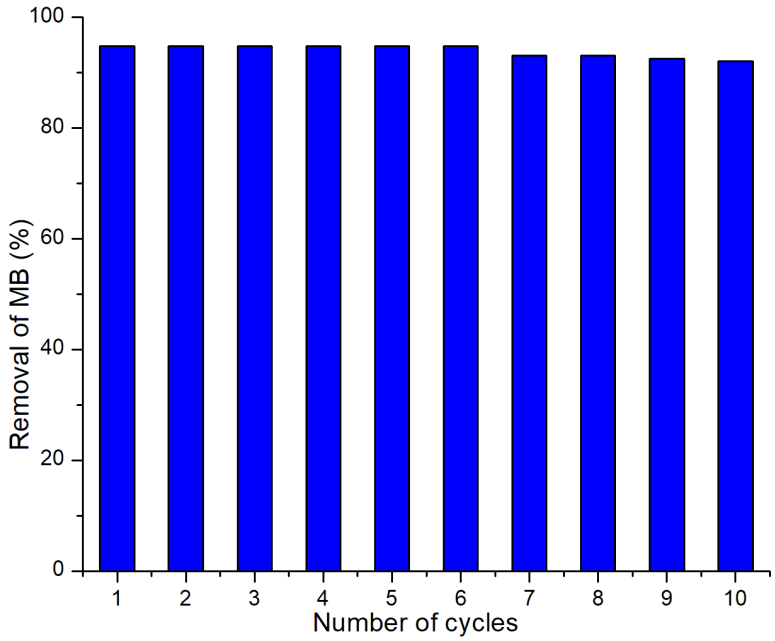

Figure V.9 Reusability of **9** on MB removal (25mL, 5 ppm MB solution with 0.1g **9**, stirred for 40 minutes).

V.4.3 Adsorption isotherms

Adsorption isotherms provide information on the amount of dye adsorbed onto the surface of the adsorbent, the adsorption capacity, multilayer or monolayer formation, and type of interaction in between the adsorbate and adsorbent. Therefore, in this study, Langmuir and Freundlich isotherms have been applied to evaluate the adsorption capacity of the CTAB-PMO solid.

V.4.3.1 Langmuir isotherm

Langmuir isotherm model predicts monolayer coverage of the adsorbate on the outer surface of the adsorbent [33]. The applicability of the Langmuir model was evaluated from the plot of C_e/q_e against equilibrium concentration, C_e for MB (Figure V.10). Q_{max} and Langmuir isotherm constant, b was evaluated from the slope and the intercept of the plot. Langmuir isotherm parameters obtained from the respective linear plot (Figure

V.10) and correlation coefficient are presented in Table V.1. The value of R^2 was only 0.703 which indicated that adsorption process does not follow Langmuir isotherm model and also the adsorption was not limited to monolayer coverage.

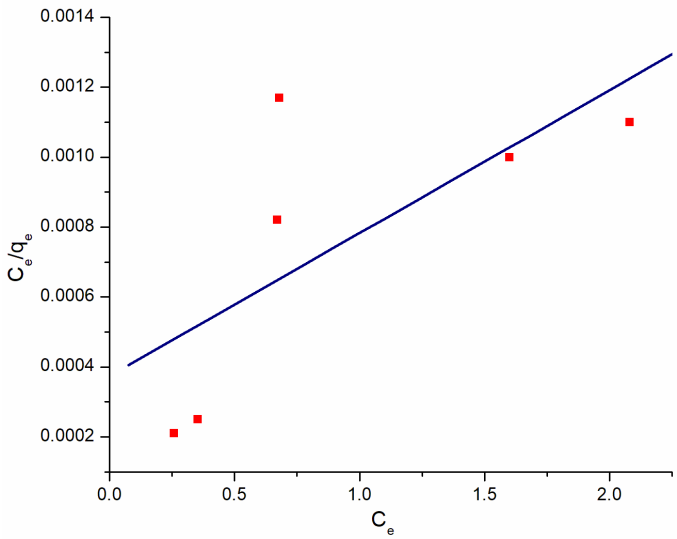

Figure V.10 Langmuir isotherm plot of dye adsorption on **9** at room temperature (adsorbent dosage = 0.1g, stirring time = 40 minutes).

Table V.1 Langmuir isotherm parameters of dye adsorption on **9**.

Q_{max} (mg/g)	R_L	Langmuir constant (b) (L/mg)	R^2
244.6	0.179	0.00914	0.703

V.4.3.2 Freundlich isotherm

The applicability of the Freundlich isotherm model was studied by plotting log q_e against log C_e which gave a straight line as shown in Figure V.11. The slope and the intercept of the plot gave the value of 1/n and K_f and are tabulated in Table V.2. Freundlich isotherm provided better regression analysis with R^2 = 0.992 (Table V.2) than Langmuir model (R^2 = 0.703). The value of n also indicated a heterogeneous nature of the surface. Therefore,

it can be inferred that adsorption of MB onto surface of **9** corresponds to multilayered heterogeneous adsorption.

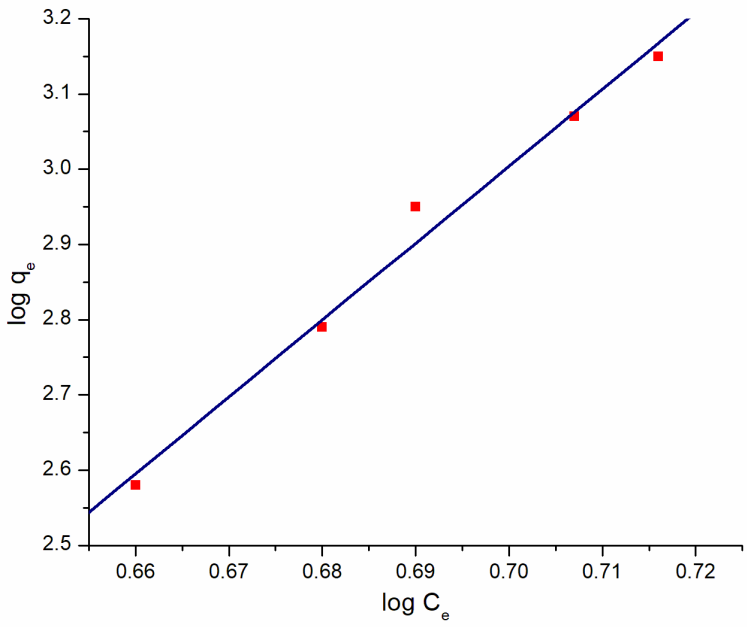

Figure V.11 Freundlich isotherm plot of dye adsorption on **9** at room temperature (adsorbent dosage = 0.1g, stirring time = 40 minutes).

Table V.2 Freundlich isotherm parameters of dye adsorption on **9**.

K_f	n	R^2
0.0071	0.097	0.992

V.4.4 Adsorption kinetics

The adsorption kinetics of MB removal was studied using the pseudo first-order, pseudo second-order and intra-particle diffusion models.

V.4.4.1 Pseudo first-order model

The values of ln (q_e-q_t) were linearly correlated with t from which k_1 and predicted q_e can be calculated using the slope and intercept of the plot. Figure V.12 represents the pseudo-

first order kinetic plot for MB adsorption by solid, **9**. The kinetic parameters obtained for the adsorption of MB on **9** have been listed in Table V.3.

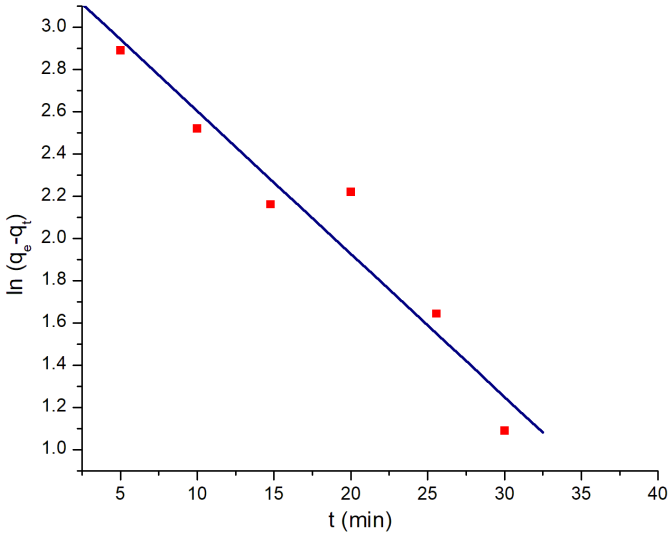

Figure V.12 The pseudo-first order kinetic model for MB adsorption by **9** (25 mL of 5 ppm MB, adsorbent dosage = 0.1g, stirring time = 40 minutes).

Table V.3 Kinetics constants and parameters determined using pseudo first-order model for the adsorption process.

K_1 (min^{-1})	q_e (graph) (mg/g)	q_e (exp) (mg/g)	R^2
0.0676	26.56	228	0.965

The value of the correlation coefficient, R^2 was 0.965 (Table V.3) and the calculated q_e value obtained from the graph (Figure V.12) was very low when compared with the experimental q_e value. Hence, it can be inferred that the MB adsorption by **9** did not adhere to the pseudo-first order kinetic model.

V.4.4.2 Pseudo second-order model

The pseudo second-order kinetics were studied by plotting t/q_t versus t which gave a straight line with slope $1/q_e$ and intercept $1/k_2q_e$. Figure V.13 represents the pseudo second-order kinetic plot for MB adsorption by solid, **9**. The kinetic parameters obtained from the plot have been listed in Table V.4.

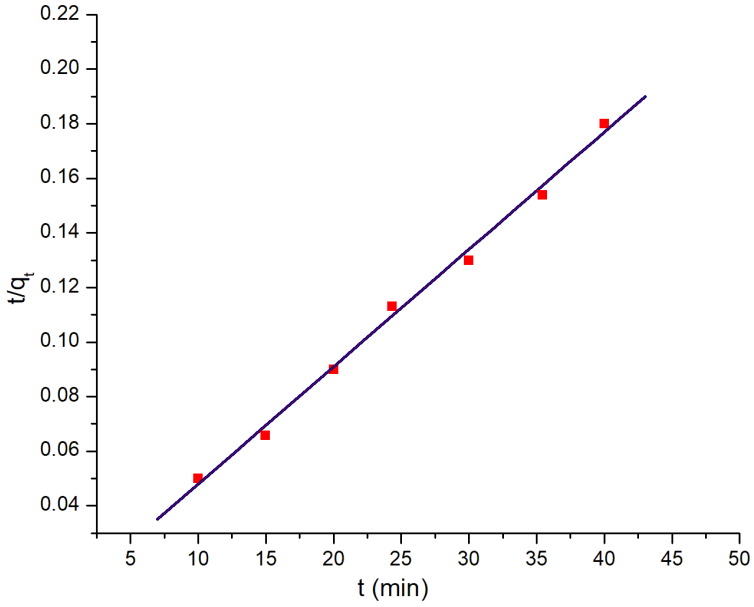

Figure V.13 The pseudo- second order kinetic model for MB adsorption by PMO solid (25 mL of 5 ppm MB and PMO dosage = 0.1g).

Table V.4 Kinetics constants and parameters determined using pseudo-second order model for the adsorption process.

K_2 (g/mg/min)	q_e (graph) (mg/g)	q_e (exp) (mg/g)	R^2
0.860	232	228	0.996

Table V.4 shows that the experimental and calculated q_e values were comparable. Moreover, the value of the correlation coefficient is nearly unity (R^2 = 0.99). Therefore,

it can be concluded that kinetic mechanism of MB adsorption by **9** follows the pseudo-second-order model.

V.4.4.3 Intra-particle diffusion model

The applicability of the intra-particle diffusion model on the adsorption of MB by **9** was evaluated by plotting a graph between q_t and the square root of time ($t^{1/2}$) as shown in Figure V.14. K_{diff} (mg g^{-1} $min^{-1/2}$) is the rate constant of the intra-particle diffusion obtained from the slope and C (mg g^{-1}) is constant found from the intercept of the plot drawn between q_t and $t^{1/2}$. Table V.5 shows the values of kinetic constants and parameters determined using intra-particle diffusion plot.

Table V.5 Kinetics constants and parameters determined using intra-particle diffusion model for the adsorption process.

K_{diff} (mg g^{-1} $min^{-1/2}$)	C (mg g^{-1})	R^2
3.536	204.37	0.970

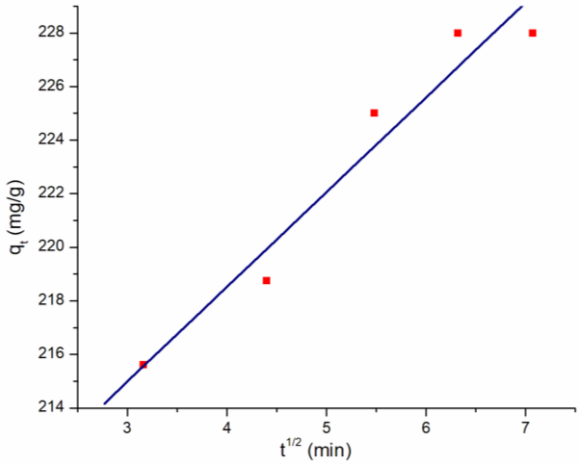

Figure V.14 The intra-particle diffusion model for MB adsorption by PMO solid (25 mL of 5 ppm MB and PMO dosage = 0.1g).

According to this model, the intra-particle diffusion is the rate-limiting step when the plot passes through the origin (as C equals to zero) [32]. As shown in Figure V.14, q_t versus $t^{1/2}$ resulted in a linear plot and regression analysis showed the value of correlation coefficient, R^2 = 0.97 (Table V.5). However, the plot did not pass through the origin indicating that the adsorption of MB onto **9** was not diffusion controlled.

V.4.5 Mechanism

Based on the experimental results, it seems that the fundamental mechanism of adsorption of dyes by solid **9** involves electrostatic interactions. Cationic dyes such as MB and MG could be strongly adsorbed onto the negatively charged surface of solid **9** via electrostatic attraction. A schematic representation of adsorption of MB by solid **9** is shown in figure V.15. However, repulsive electrostatic interactions become dominant between anionic dyes and solid **9**, which resulted in their poor adsorption.

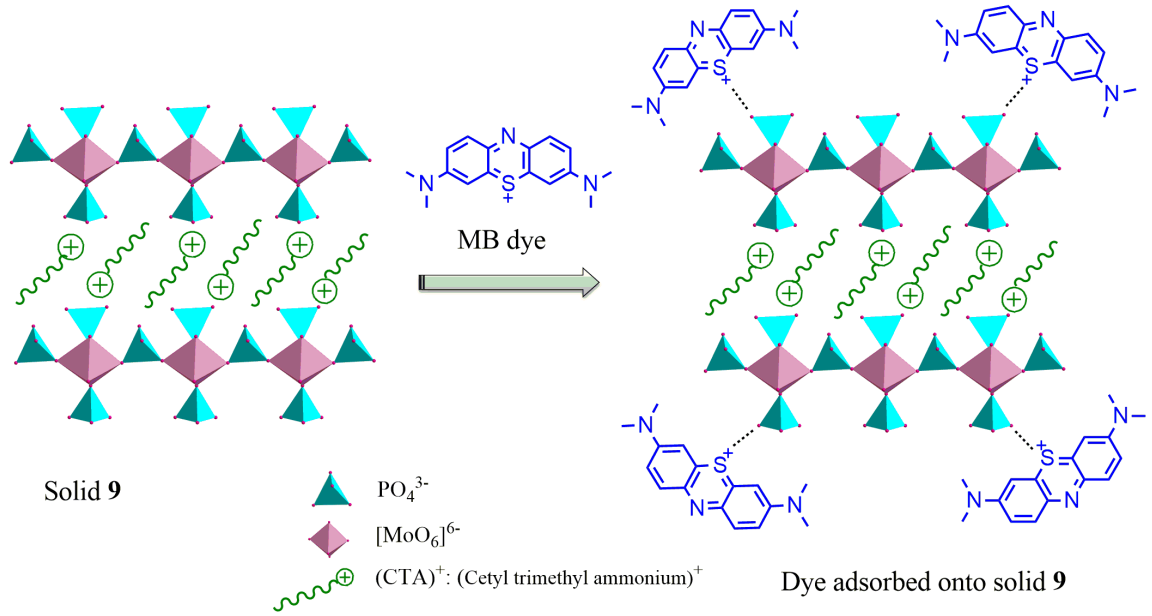

Figure V.15 Adsorption of MB onto the surface of solid **9** via electrostatic attraction.

V.5 Conclusion

Nanostructured phosphomolybdate solid templated by cationic surfactant, CTAB was synthesized under ambient conditions and characterized. The synthesized hybrid was investigated for its efficiency in removing cationic and anionic dyes from aqueous solution. The solid, **9** was found to be effective adsorbent in removing cationic dyes *viz*; methylene blue and malachite green. The maximum removal efficiency of 94.8 % was achieved on treating 25mL of 5ppm MB solution with 0.1g of **9** for 40 minutes. The solid **9** could be reused upto 6 cycles without any loss in adsorption efficiency. The equilibrium adsorption data was best modeled using the Freundlich isotherm and the pseudo second-order kinetic model provided the best correlation for the experimental data. CTAB templated PMO nanoparticles appear to be a promising novel adsorbent for selective removal of cationic dyes in effluent treatment process.

References

1. Parker A (1932) Nature 130:761-763

2. Huang Z, Li Y, Chen W, Shi J, Zhang N, Wang X, Li Z, Gao L, Zhang Y (2017) Mater Chem Phys 202:266-276

3. Malarvizhi R, Ho YS (2010) Desalination 264:97-101

4. Katheresan V, Kansedo J, Lau SY (2016) J Environ Chem Eng 6:4676-4697

5. Tian X, Hou L, Wang J, Xin X, Zhang H, Ma Y, Wang Y, Zhang L, Han Z (2018) Dalton Trans 47:15121-15130

6. Ali I, Peng C, Naz I, Lin D, Saroj D P, Ali M (2019) RSC Adv 9:3625-3646

7. Khan MI, Akhtar S, Zafar S, Shaheen A, Khan MA, Luque R, Rehman A (2015) Materials 8:4147-4161

8. Ahmad A, Setaper SHM, Chuo SC, Khatoon A, Wani WA, Kumar R, Rafatullah M (2015) RSC Adv 5:30801-30818

9. Erdemoglu S, Aksu SK, Sayilkan F, Izgi B, Asilturk M, Sayilkan H, Frimmel F, Gucer S (2008) J Hazard Mater 155:469-476

10. Wang S, Li H, Xu L (2006) J Colloid Interface Sci 295:71-78

11. Liu L, Lin Y, Liu Y, Zhu H, He Q (2013) J Chem Eng Data 58:2248-2253

12. Hameed BH, El-Khaiary MI (2008) J Hazard Mater 154:639-648

13. Kausar A, Iqbal M, Javed A, Aftab K, Nazli Z, Bhatti HN, Noureen S (2018) J Mol Liq 256:395-407

14. Yao L, Lua SK, Zhang L, Wang R, Dong ZL (2014) J. Hazard. Mater 280:428-435

15. Kaur J, Kozhevnikov IV (2004) Catal Commun 5:709-713

16. Li HL, Qi W, Li W, Sun H, Bu WF, Wu LX (2005) Adv Mater 17:2688-2692

17. Wang XL, Wang YH, Hu CW, Wang EB (2002) Mater Lett 56:305-311

18. Kurth DG, Lehmann P, Volkmer D, Coelfen H, Koop MJ, Muller A, Du Chesne A (2000) Chem Eur J 6:385-393

19. Kurth DG, Lehmann P, Volkmer D, Muller A, Schwahn D (2000) J Chem Soc Dalton Trans 21:3989-3998

20. Volkmer D, DuChesne A, Kurth DG, Schnablegger H, Lehmann P, Koop MJ, Muller A (2000) J Am Chem Soc122:1995-1998

21. Wu P, Volkmer D, Bredenkotter B, Kurth DG, Rabe JP (2008) Langmuir 24:2739-2745

22. Thomas J, Kannan KR, Ramanan A (2008) J Chem Sci 120(6):529-536

23. Huo Q, Margolese DI, Ciesla U, Demuth DG, Feng P, Gier TE, Sieger P, Firouzi A, Chmelka, BF, Schüth F, Stucky GD (1994) Chem Mater 6:1176-1191

24. Yamauchi Y, Kuroda K (2008) Chem Asian J 3:664-676

25. Bu W, Li W, Li H, Wu L, Tang AC (2004) J Colloid Interface Sci 274:200-203

26. Tang ZY, Liu SQ, Wang EK, Dong SJ, Wang EB (2000) Langmuir 16:5806-5813

27. Zhang G, Ke H, He T, Xiao D, Chen Z, Yang W, Yao J (2004) J Mater Res 19:496-500

28. Langmuir I (1918) J Am Chem Soc 40(9):1361-1403

29. Freundlich HMF (1906) Z Phys Chem 57A:385-470

30. Lagergren S (1898) K Sven Vetensk Handl 24(4):1-39

31. Ho YS, McKay G (1999) Process Biochem 34(5):451-465

32. Weber WJ, Morris JC (1963) J Sanit Eng Div Am Soc Civil Eng 89:31-60